A Miniature Distributed Ku-Band Phase Shifter Using Tunable Inductors and MEMS Varactors

Feng Lin, Muzhi Wang, and Mina Rais-Zadeh*, *Senior Member, IEEE*
Department of Electrical Engineering and Computer Science, University of Michigan, Ann Arbor, MI 48109 USA
*minar@umich.edu

Abstract- **This work reports on a miniature distributed microelectromechanical system (MEMS) phase shifter using both tunable capacitors and inductors. Compared to the conventional distributed MEMS phase shifters with only tunable capacitors, the proposed MEMS phase shifter has one more design parameter (tunable inductor value) to realize high return loss of more than 26 dB at all states, large phase shift of 37.5°/mm per unit length, and large phase shift per decibel of 180°/dB at 15 GHz. A one proof-of-concept 1 bit phase shifter is fabricated and characterized. The measured results of the phase shifter are in good agreement with measurements.**

I. Introduction

Advances in software defined radio and cognitive radio demand reconfigurable RF front-end components to support different frequencies and communication standards. Such systems can offer smaller size at a lower cost compared to conventional single-frequency radios. As a main component of phased-array antennas, microwave and millimeter-wave phase shifters are required to be low loss, widely tunable (broadband), low power, small size, and fast. In addition, phase shifters are required to handle high RF powers when used in the transmit channels or in radars for beam-forming applications.

RF MEMS switches have been extensively used in the design of microwave and mm-wave phase shifters, as they offer several advantages, such as low power consumption and high linearity, compared to traditional p-i-n diodes and field effect transistor (FET) switches [1]. There are mainly four kinds of MEMS shifters: reflect-line, switched-line, loaded line and distributed MEMS transmission line (DMTL). Due to the true-time-delay (TTD) (*i.e.*, linear phase versus frequency) and broad-band operation properties, many papers on the DMTL [1]-[4] have been published since it was proposed by Barker and Rebeiz [2]. The DMTL usually consists of a high-impedance coplanar waveguide (CPW) transmission line that is periodically loaded by MEMS switches as shown in Fig. 1 (a). Fig. 1 (b) shows the equivalent circuit of the DMTL unit.

The MEMS switches are used to increase the loading capacitance in the down state, which realizes a differential phase shift with respect to the phase in the up state. The phase constant β and characteristic impedance in the down state of the MEMS switch are calculated as

$$\beta_{down} = \sqrt{sL_t(sC_t + C_{MEMS\_down})}\ , \tag{1a}$$

$$Z_{down} = \sqrt{\frac{sL_t}{sC_t + C_{MEMS\_down}}}\ , \tag{1b}$$

where s is the length of the phase shifter unit, L_t and C_t are per unit inductance and capacitance of the unloaded line. C_{MEMS_down} is the value of the MEMS switch at the down state, defined by the thickness of the dielectric layer and overlap area of the electrodes.

Equation (1) indicates that to get a larger phase shift per unit (*i.e.*, larger β), one should increase the value of C_{MEMS_down}, which results in a lower impedance Z_{down} and thus deteriorated matching condition. Therefore, the conventional DMTL cannot realize large phase shift and good matching, simultaneously. To overcome this limitation of conventional DMTL that usually includes only tunable capacitors, a phase shifter with both tunable inductors and capacitors is proposed. When increasing C_{MEMS_down} to obtain a large phase shift, the value of tunable inductor is also increased, keeping Z_{down} matched to the port impedance while further increasing the phase shift.

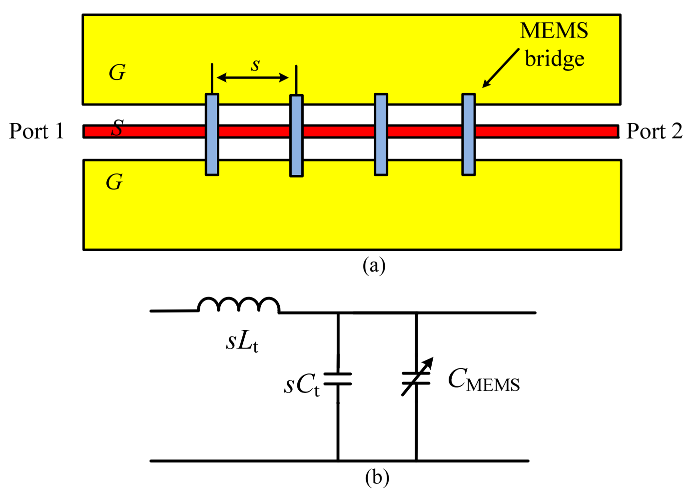

Fig. 1. (a) Structure and (b) lumped model of a conventional DMTL phase shifter. The value of L_t can be made tunable to keep the impedance matched when the capacitor is tuned.

II. Slow-Wave Distributed MEMS Phase Shifters Design Procedure and Fabrication

A. Design procedure

Fig. 2 (a) shows the unit structure of proposed DMTL phase shifter, which consists of two series ohmic-contact and one shunt capacitive MEMS switches and two metal-air-metal (MAM) capacitors. In the normal state (large propagation velocity state), the series switches are pulled in, while the shunt switch is not activated. The series switch is modeled as a section of a low-impedance transmission line as shown in Fig. 2 (b). The characteristic impedance of the loaded line for this state is designed to be 50 Ω. In the slow-wave state (small propagation velocity state), the series switches are not activated, while the shunt switch is pulled in. When the series switch is off, the narrow, high-impedance transmission line is molded as a series inductor $L_s/2$ (Fig 2. (c)). As the series inductance and shunt capacitance are simultaneously increased, the characteristic impedance of the phase shifter for this state is maintained matched to 50 Ω (the termination impedance).

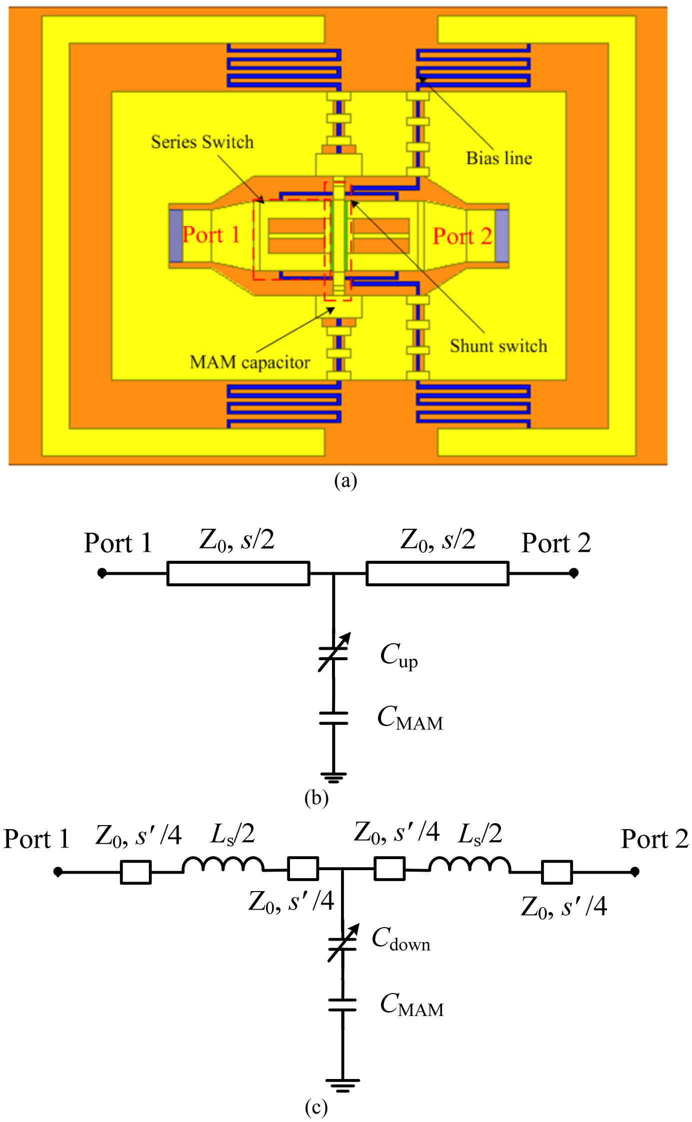

Fig. 2. The (a) structure, and (b) lumped model in the normal state and (c) in the slow-wave state for the presented DMTL phase shifter.

Fig. 3 (a) and (b) show the structures of series and shunt switches. The COMSOL simulation results show that the pull-in voltages for the series switch and shunt switch are 17.5 V and 33.5 V, respectively, assuming an initial air gap of 1.8 μm.

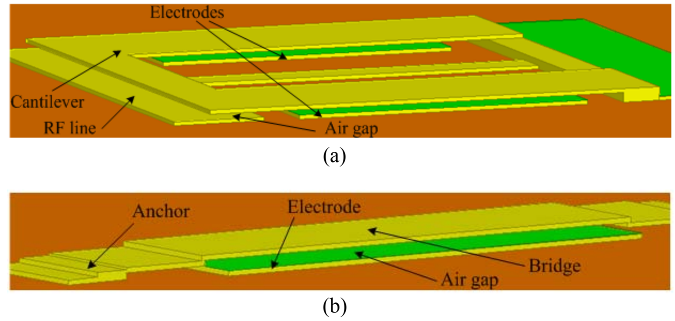

Fig. 3. The (a) structure of the series and (b) shunt switches.

B. Fabrication process

The phase shifter is fabricated on a 500 μm thick quartz substrate (ε_r=3.8, tan δ=0.00002 at 10 KHz). Table I(i)–(vi) shows the surface micromachining fabrication process flow. (i) The process begins with 1200 Å thick TiN resistive layer deposition by sputtering and patterning by lift-off to form the bias lines. (ii) The next step is the evaporation of a 200 Å /5000 Å thick Cr/Au layer, which is patterned by lift-off to form the MEMS switch bottom electrode and the phase shifter first gold layer. (iii) A 1500 Å thick Si3N4 layer is coated using plasma enhanced chemical vapor deposition technique (PECVD) and patterned using the reactive ion etching (RIE) technique to form the dielectric layer. (iv) Next, a sacrificial layer (PMMA) with a thickness of 1.6 μm is deposited and patterned using RIE technique with evaporated Cr (1000 Å) as a mask layer. (v) A seed Cr/Au layer (200 Å /1000 Å) is evaporated and 2 μm Au is electroplated to form the cantilevers, bridges and the phase shifter top metal. (vi) The sacrificial layer is wet released and dried in a critical point dryer. Fig. 4 shows the scanning electron microscope (SEM) photograph of one unit cell of phase shifter fabricated using the process flow described in Section II.

TABLE I
FABRICATION PROCESS OF THE PHASE SHIFTER

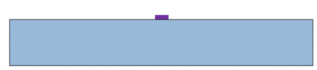 (i) Deposit and pattern TiN on a silica wafer	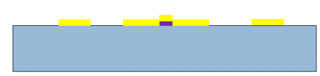 (ii) Lift-off pattern Cr/Au bottom electrode
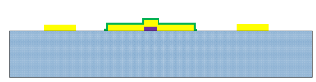 (iii) Deposit PECVD silicon nitride and pattern with RIE	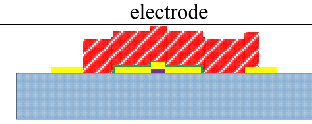 (iv) Sacrificial layer deposition and patterning with RIE
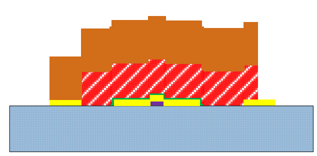 (v) Electroplate Au	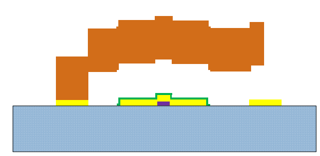 (vi) Etch sacrificial layer and release
Sputtered TiN, PECVD Si_3N_4, Electroplated Au, Evaporated Au, PMMA, Quartz substrate	

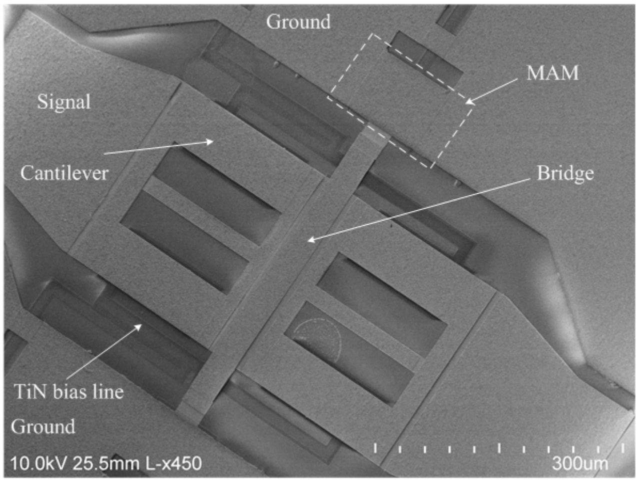

(a)

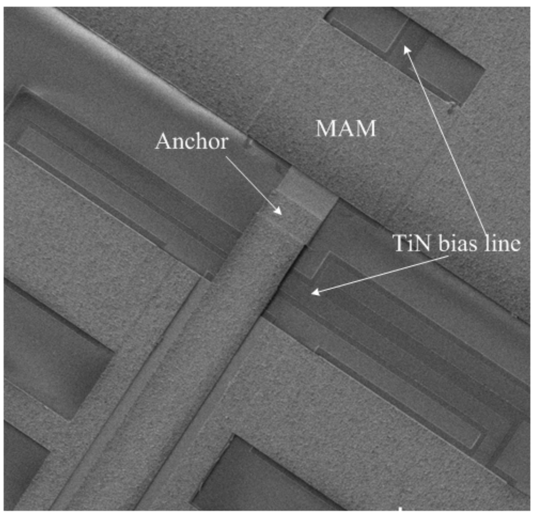

(b)

Fig. 4. The SEM images of (a) one-unit cell of the phase-shifter structure and (b) detailed view of the anchor region of the shunt switch.

III. Results

A. 1 unit phase shifter performance

On-wafer measurements are carried out using N5214A Agilent PNA-X network analyzer and Cascade Microtech GSG ACP-probes. A thru-reflect-line (TRL) calibration was performed prior to measurements and bias tees were used to protect the PNA. DC bias was applied using DC probes to the TiN bias lines.

The *S*-parameters of the unit cell of the phase shifter (one bit) with maximum phase shift of 24.5° are shown in Fig. 5 for the normal and the slow-wave states. It can be observed that both states have a return loss of better than 20 dB, with a worst-case insertion loss of 0.5 dB at 15 GHz. The actual up state capacitance value of shunt switch is increased because of the reduced air gap after release. While the actual downstate capacitance value of shunt switch is lower than the simulated value due to the increased actual dielectric layer thickness and the bridge surface roughness. It reduces unit cell phase shift performance of the measured phase shifter to 15.5° as compared to design value of 24.5° for the phase shifter at 15 GHz. The simulated response with measured nitride thickness of 0.27 µm and assumed air gap of 1.2 µm is also overlaid in Fig. 5 for comparison. Note that the measured PMMA thickness is ~1.6µm. After release, the air gap may be reduced. The value of 1.2 µm provides the best fit to measured results.

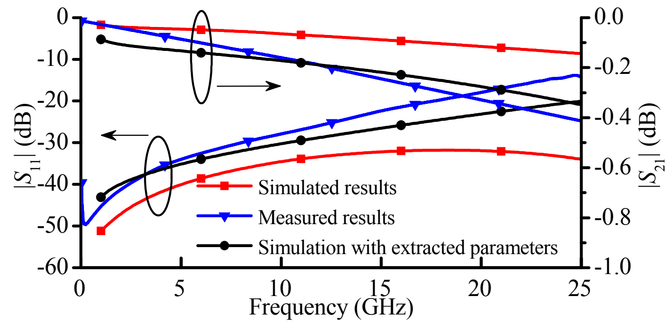

(a)

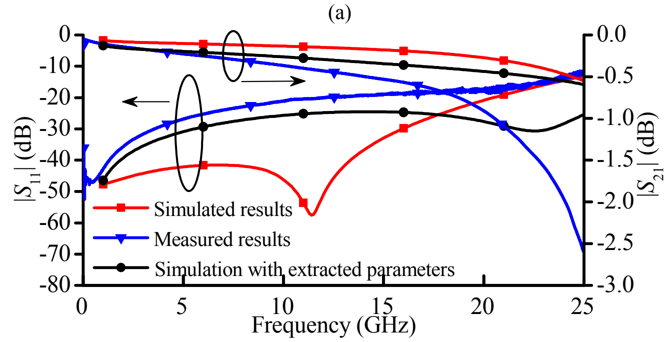

(b)

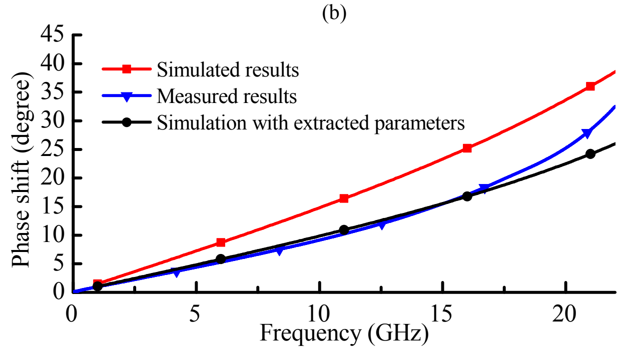

(c)

Fig. 5. *S*-parameters for (a) normal state and (b) slow-wave state and (c) phase shift of the 1-section 22.5° DMTL phase shifter.

B. Two-bit 12 units phase shifter performance

Fig. 6(a) shows the layout of a 2-bit 12-section 270° DMTL phase shifter for Ku-band (f_0=15 GHz) applications. The S-parameters and phase shift of the device at different stated of the series and shunt switches are shown in Figs. 6 (b) and (c). Depending on the state of the switches, discrete phase shifts of 90°, 180°, and 270° are achieved at 15 GHz. As shown, by utilizing both tunable inductors and capacitors, the return loss is better than 26 dB for all states and the worst case insertion loss is 1.5 dB

Table II compares the performance specifications of the proposed phase shifter with reported phase shifters in a similar frequency range. As shown, the proposed phase shifter compares well or even outperforms the reported phase shifters in terms of return loss performance and unit size.

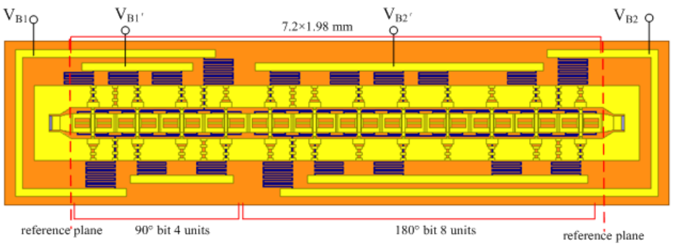

(a)

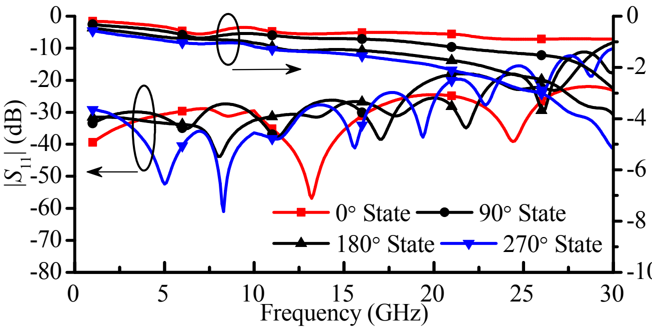

(b)

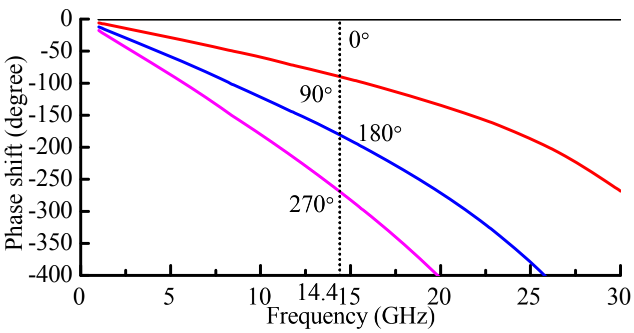

(c)

Fig. 5. (a) Layout of the 2-bit 12-section 270° DMTL phase shifter. (b) *S*-parameters and (c) phase shift for all states.

TABLE II
PERFORMANCE COMPARISONS OF THE PROPOSED DMTL PHASE SHIFTERS WITH OTHER MEMS PHASE SHIFTERS IN A SIMILAR FREQUENCY RANGE

	T-MTT [3]	T-MTT [4]	This paper
Center frequency (GHz)	13.6	30	15
Return loss (dB)	>12.5	>25	>25.6
Insertion loss (dB)	0.9-1.6	0.75-1.15	0.66-1.47
Phase shift range (°)	0-270	0-225	0-270
Phase shift/unit (°)	12.8	22.5	22.5
Unit length (μm)	1150	460	600
Substrate	Quartz	Quartz	Quartz

IV. CONCLUSION

A new miniature distributed MEMS phase shifter was introduced. The design takes advantage of both tunable capacitors and tunable inductors to realize large phase shift per unit without deteriorating the matching condition. Simulated and measured results of proof-of-concept devices were in good reasonable. The same concept can be applied to implement high-performance and high power handling phase shifters using phase change RF switches such as those demonstrated in [5].

V. ACKNOWLEDGEMENT

This work is partially supported by the NSF Enhancing Access to the Ratio Spectrum (EARS) program and partially by NSF CAREER program.

REFERENCES

[1] G. M. Rebeiz, K. Entesari, I. Reines, S.-J. Park, M. A. El-Tanani, A. Grichener, and A. R. Brown, "Tuning in to RF MEMS," *IEEE Microw. Mag.*, vol. 10, no. 5, pp. 55–72, Oct. 2009.

[2] S. Barker and G. Rebeiz, "Distributed MEMS true-time delay phase shifters and wide-band switches," *IEEE Trans. Microw. Theory Tech.*, vol. 46, no. 11, pp. 1881–1889, Nov. 1998.

[3] J. S. Hayden and G. Rebeiz, "Very low-loss distributed X -band and Ka -band MEMS phase shifters using metal–air–metal capacitors," *IEEE Trans. Microw. Theory Tech.*, vol. 51, no. 1, pp. 309–314, Jan. 2003.

[4] B. Lakshminarayanan and T. Weller, "Design and modeling of 4-bit slow-wave MEMS phase shifters," *IEEE Trans. Microw. Theory Tech.*, vol. 54, no. 1, pp. 120–127, Jan. 2006.

[5] Y. Shim, G. Hummel, and M. Rais-Zadeh, "RF switches using phase change materials," *in Proc. IEEE MEMS Conf.*, Jan. 2013, pp. 237–240.